

Stator Ground Protection for Multiple High-Impedance Grounded Generators Sharing a Common Bus

Ritwik Chowdhury, Dale Finney, Normann Fischer,
Jason Young, Veselin Skendzic, and Subhash Patel
Schweitzer Engineering Laboratories, Inc.

Presented at the
74th Annual Georgia Tech Protective Relaying Conference
Virtual Format
April 28–30, 2021

Published in
*Synchronous Generator Protection and Control: A Collection of
Technical Papers Representing Modern Solutions, 2019*

Originally presented at the
45th Annual Western Protective Relay Conference, October 2018

Stator Ground Protection for Multiple High-Impedance Grounded Generators Sharing a Common Bus

Ritwik Chowdhury, Dale Finney, Normann Fischer, Jason Young, Veselin Skendzic, and Subhash Patel,
Schweitzer Engineering Laboratories, Inc.

Abstract—Typical 100 percent stator ground protection for a single high-impedance grounded generating unit involves using a neutral overvoltage element in conjunction with a third-harmonic or injection scheme. Both of the latter schemes face reliability challenges when applied to multiple high-impedance grounded generators that share a common bus or generator step-up winding.

Third-harmonic schemes cannot be applied to protect the neutral end due to the possibility of circulating third-harmonic contributions from the paralleled units. In addition, the change in the impedance network when units share a bus can result in third-harmonic scheme misoperation. This paper presents a method that secures the third-harmonic scheme when misoperation is a possibility.

When injection schemes are applied, the paralleled units appear as a ground fault to the protected unit. Addressing this requires desensitizing the element and thereby making it ineffective. This paper discusses a method to account for the grounding sources from the paralleled units to allow sensitive and secure injection scheme application.

Another challenge for ground fault protection is a lack of selectivity when protecting units that share a bus. This paper presents two complementary methods that facilitate selectivity. One method compares fundamental and third-harmonic voltages to determine the faulted unit. The other method leverages sensitive current inputs available in modern relays. Using communications, both of these methods can be used to bias the conventional staggered tripping scheme to achieve a selective breaker trip.

I. INTRODUCTION

There are two main reasons for providing 100 percent stator ground protection. First, a ground fault can occur anywhere in the winding. Ground faults are normally due to deterioration of the winding insulation [1], so if a ground fault occurs, there is an increased likelihood of a second fault. If a fault occurs at or near the neutral and goes undetected, a second fault elsewhere in the winding will not be limited by the neutral grounding resistor (NGR) and the resulting damage could be very high. Applying 100 percent stator ground protection guards against this possibility.

Second, a series fault can occur due to a fractured stator bar. This type of fault can also be very damaging. It cannot be detected by the functions that normally protect the stator winding and may only be detected once the fault burns through the ground-wall insulation and arcs to ground [2]. The application of 100 percent stator ground protection is therefore needed for possible series faults at the generator neutral.

High-impedance grounded generators have been successfully protected by 100 percent stator ground protection schemes for many years. These schemes take advantage of the fact that the zero-sequence network of the generator is normally isolated from the rest of the system by the delta windings of the generator step-up transformer (GSU) and unit auxiliary transformer (AUX). However, there are several instances where alternate system configurations create application challenges:

- **Multiple high-impedance grounded generators sharing a single GSU.** In this case, several small generators are connected to a common bus, each through its own breaker. A single GSU connects this bus to the system. Each generator is high-impedance grounded. There are real-world systems with up to five generators in such a configuration.
- **Multiple ungrounded generators sharing a GSU with a high-impedance grounding source on the bus.** Similar to the previous configuration, several small generators are connected to a common bus, each through its own breaker. A single GSU connects this bus to the system. Each generator is ungrounded. A grounding transformer on the bus provides a ground source for all the units. This is an economical configuration, although not operationally ideal because offline generators become ungrounded.
- **Cross-compound units.** These are typically large steam units where the high-pressure (HP) and low-pressure (LP) turbines are mounted on different shafts. Often, the HP turbine drives a 2-pole generator at 3,600 rpm and the LP turbine drives a 4-pole generator at 1,800 rpm. The two generators share the same GSU. There are usually no breakers, but in some cases the LP generator has a disconnect switch. The HP generator neutral is high-impedance grounded, and the LP generator neutral is ungrounded.

The first two configurations are relatively common for hydroelectric generating stations. For example, one utility in the United States has 154 high-impedance grounded generators, 73 (47.4 percent) of which are on shared buses.

Generally, the strength of the grounding source dictates the ground fault protection method. In low-impedance grounded systems, the ground fault current is relatively high and the neutral voltage during a fault is relatively low. However, in high-impedance grounded systems, the situation is the opposite.

Hence, current-based ground fault protection schemes are usually applied in low-impedance systems, whereas voltage-based schemes are applied in high-impedance systems.

For protecting a single high-impedance grounded generator, the neutral overvoltage element (59N) is the workhorse. It responds to the fundamental frequency voltage measured across the NGR. It can also be applied at the machine terminals via a derived zero-sequence voltage (in a digital relay) measured by a wye-grounded or broken-delta PT. This simple function detects ground faults on the stator winding, isolated phase bus, and GSU and AUX delta windings. Since the zero-sequence voltage is virtually the same everywhere, the 59N element cannot determine the location of the fault within the zero-sequence network. In the system shown in Fig. 1, a 59N element can be applied at the neutral of each generator. However, both elements will operate for a ground on either machine, making it difficult to selectively trip either Breaker A or B.

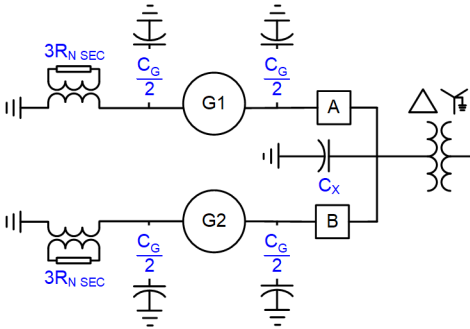


Fig. 1. Two high-impedance grounded generators sharing a common bus

The 59N element can find faults on 90 to 95 percent of the stator winding, but it leaves the 5 to 10 percent of the winding nearest the neutral point vulnerable. Another scheme is needed to provide 100 percent coverage. An injection scheme (64S) is one such element. It detects ground faults by injecting a signal across the grounding resistor into the generator stator and measuring the resulting current. The injected signal is ac, so it can be coupled through a transformer to the primary circuit. The signal must be zero-sequence so that it is confined by the delta windings of the GSU and AUX.

The signal is usually a subharmonic of the fundamental frequency; however, this is not always the case. Recently, schemes that inject signals with multiple frequencies have become available [3]. The basic operating principle is that of an ohmmeter. Under unfaulted conditions, current flows only through the zero-sequence system capacitances. The current is small due to the low frequency, and the measured impedance is high. A ground fault causes an increase in current that reduces the impedance measurement. Some schemes provide increased sensitivity by resolving the measurement into its resistive and capacitive components.

Considering Fig. 1, an injection scheme can be connected at the neutral of G1. The neutral connection of G2 provides an additional path for the injected current, which reduces scheme sensitivity. This injection scheme responds to faults on both machines if both generator breakers are closed. To provide coverage when a breaker is open, an injection unit can be

applied at the neutral of each generator. However, this is not a recommended approach when using conventional implementations that inject a single frequency signal due to security concerns.

The third-harmonic scheme is another method used to provide coverage for the last 5 to 10 percent of the winding. It can be thought of as a form of injection scheme where the injection source is the generator itself. Notably, most synchronous generators produce a significant third-harmonic voltage. The third harmonic behaves like a zero-sequence component. It is confined by the GSU and AUX delta windings. However, the level of third harmonic produced by a generator is variable and often difficult to characterize.

There are two third-harmonic scheme variations: third-harmonic undervoltage and third-harmonic comparison. The former operates on the neutral third-harmonic voltage and can be applied to systems that do not have grounded-wye or broken-delta PTs at the machine terminals; however, it is difficult to set, less secure than the latter, and not within the scope of this paper. The third-harmonic comparison scheme, on the other hand, compares the third-harmonic voltage measured at the terminals and at the neutral of the generator. For a single, unfaulted generator, this comparison corresponds to a predictable voltage division in accordance with the impedances of the zero-sequence network [4].

In a system with multiple machines, such as that of Fig. 1, a third-harmonic scheme may be applied to each generator. However, the network impedances will change with the states of the breakers. Furthermore, differences in the third-harmonic levels produced by the two machines will cause the circulation of third-harmonic current between the two machines, upsetting the expected voltage ratio. This makes the application of a conventional third-harmonic scheme impractical.

II. THIRD-HARMONIC SCHEMES

A. Field Experience

The behavior of various third-harmonic schemes and the solutions to the challenges they face are covered in [4]. These schemes can be difficult to apply and were not designed to protect generators that share a common bus due to the issues mentioned in the previous section, resulting in misoperations.

One such field event is illustrated in Fig. 2.

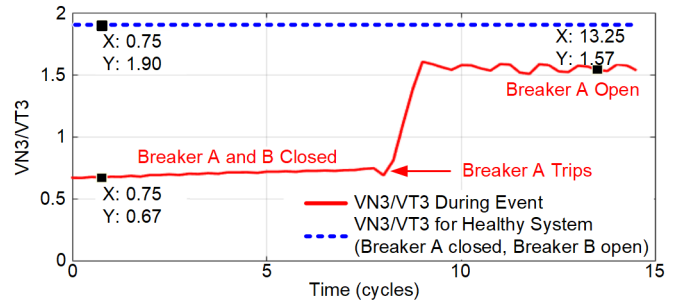


Fig. 2. Third-harmonic element behavior during an event

A 12 MVA, 13.8 kV hydroelectric unit (G1 in Fig. 1) tripped after being synchronized to a bus with an identical unit that was online. There was no ground fault on the unit, but there

was a large deviation in VN3 and VT3. This event demonstrates the issues caused by sharing a bus with another generator. The circuit changes depending on the breaker status.

If a single unit (G1) is online with Breaker A closed and Breaker B open (Fig. 3), the third-harmonic voltage produced by the generator (VG3) is the sum of the voltage drops across the terminal capacitances (VT3) and the neutral impedance (VN3). This is the circuit assumed when applying neutral-side protection via third-harmonic comparison schemes [4]. For the event of Fig. 2, the ratio of VN3/VT3 for the healthy unit-connected system is 1.90.

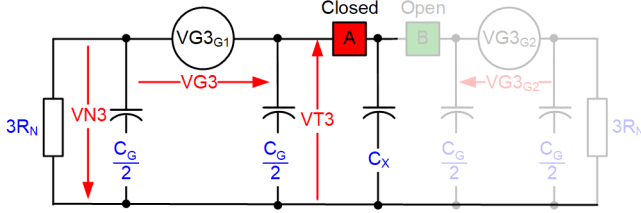


Fig. 3. Assumed circuit when applying third-harmonic comparison schemes

When Breaker A is open (Fig. 4), the terminal-side capacitance decreases (i.e., terminal impedance increases). This reduces VN3, increases VT3, and results in a lower VN3/VT3 ratio. For the event in Fig. 2, this corresponds to a ratio of 1.57.

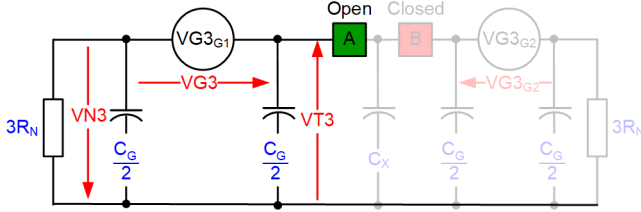


Fig. 4. Circuit with G1 offline and terminal Breaker A open

When G1 and G2 are paralleled with both Breakers A and B closed (Fig. 5), there are two competing issues.

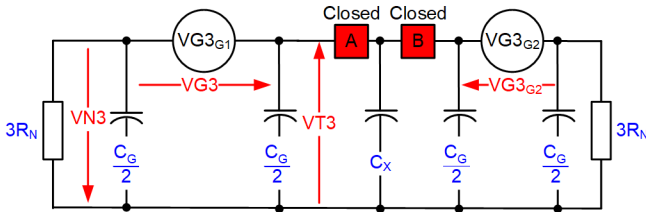


Fig. 5. Multiple paralleled units sharing a common bus

First, there are additional terminal-side impedances not in Fig. 3, such as C_G and $3R_N$, from the paralleled unit. This causes the terminal-side impedances to go down, resulting in a decrease in VT3 and an increase in VN3.

Second, the additional source VG_{3G2} may cause VT3 to increase significantly and VN3 to decrease by the same amount, proportional to VG_{3G2} . Since a generator's VG3 depends on the terminal voltage magnitude, loading, and power factor, this could result in a significant reduction of VN3/VT3. In Fig. 2,

where G2 was loaded and G1 was not (scenario of Fig. 5), this reduction was the dominant effect. The VN3/VT3 ratio of 0.67 was large enough to cause the misoperation.

Note that Fig. 5 assumes that the units sharing the bus are similar models with the same stator ground capacitance (C_G).

B. VN3/VG3 Ratio Method (64G3)

The first issue, resulting in a decreased VT3 and increased VN3, is characteristic of a fault at the machine terminals. Using a scheme that detects faults only at the neutral (and not the terminals, as is the case with some schemes [4]) solves this issue. Furthermore, due to the various operating states based on breaker statuses, it is preferable to use a scheme that is immune to the resulting impedance changes. The number of state permutations rapidly increases as more units share the bus. The third-harmonic scheme based on (1) is immune to the changes in impedance due to breaker statuses and operates for faults only at or near the machine neutral [4].

$$64G3 = \frac{VN3}{VG3} < 64G3P \quad (1)$$

64G3 operates if the third harmonic measured at the neutral is too low compared with the total third harmonic produced by the unit. The pickup, 64G3P, is set to the percentage of winding protection desired. Generally, setting it to 15 percent to obtain a 5 to 10 percent overlap with the 59N function is adequate [4]. The scheme typically includes a minimum supervision (e.g., $VG3 > 0.01$ pu of the generator nominal line-to-neutral voltage [V_{LN}]) to ensure that the generator is producing a healthy amount of third harmonic. The only requirement for this scheme to behave well is that the generator be high-impedance grounded. Based on real-world systems we have seen, a healthy 64G3 ratio for high-impedance grounded generators typically ranges from 0.40 to 0.80 and results from sizing the NGR based on the system capacitance.

The choice of the 64G3 third-harmonic scheme still does not address the second issue of circulating third harmonics from the external source adding to VT3 and subtracting from VN3. The voltages look identical to a neutral-side ground fault. One approach is to supervise the third-harmonic element with a high-set forward power element. While this helps, it is a crude approach that assumes that the third harmonic produced by a unit is a surrogate of real power. This is not always the case as power factor, along with terminal voltage, also has a significant influence on the level of third harmonic produced by a generator. If similarly loaded units have significantly different power factors, using forward power supervision can result in a misoperation.

C. Blocking Ratio Method (64G3N)

The optimal way to address security is to use a communications scheme that allows the relay to make better decisions by knowing how much third harmonic is produced by the paralleled units. This scheme is shown in Fig. 6.

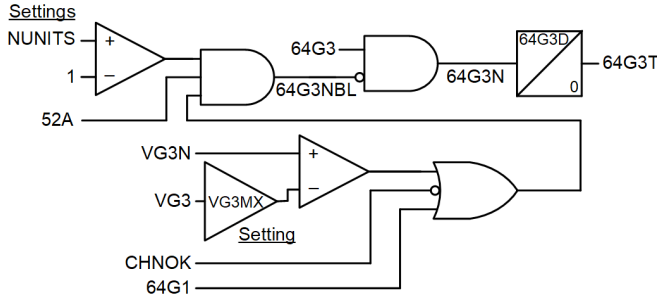


Fig. 6. Blocking ratio method (64G3N) using communications

Each relay transmits and receives VG3 (a scalar magnitude) to and from all other relays protecting units on the bus. A blocking signal (64G3NBL) is generated if there is a possible misoperation, which can occur in the following circumstances:

- Any of the other units in the system produces a large amount of third harmonic (VG3N) relative to the protected unit (VG3 multiplied by VG3MX).
- The communications channel is not healthy or invalid data are received (not CHNOK).
- The fundamental neutral overvoltage element (64G1 in Fig. 6) picks up and then is relied on for dependability.

The blocking signal (64G3NBL) is only generated if there is more than one generator in the protected system ($NUNITS > 1$) and the protected unit shares the bus (52A is asserted).

This method is simple and exhibits good availability when the VG3 produced by the protected unit is not significantly less than that of the other units. This could be the case if the units sharing the bus are similar models (in terms of ratings, winding functions, pole shapes, and so on) and are loaded similarly for both real and reactive power. This is most often the case for hydroelectric units. Various low-bandwidth communications schemes can be used, such as IEC 61850 GOOSE, synchrophasors, hardwired transducer I/O, or a proprietary protocol.

The VG3MX setting can be obtained by evaluating the zero-sequence network for the system under consideration. For the two-unit example of Fig. 1, the $64G3_{RATIO}$ value corresponding to one unit online (Fig. 3) is shown in (2).

$$64G3_{RATIO} = \frac{\frac{C_G}{2} + C_X}{C_G + \frac{1}{3j\omega R_N} + C_X} \quad (2)$$

$$64G3N_{RATIO} = \frac{\frac{C_G}{2} + C_X + (N-1)\left(C_G + \frac{1}{3j\omega R_N}\right)}{N\left(C_G + \frac{1}{3j\omega R_N}\right) + C_X} - \sum_{n=2}^N \frac{VG3_n}{VG3} \frac{\left(\frac{C_G}{2} + \frac{1}{3j\omega R_N}\right)}{N\left(C_G + \frac{1}{3j\omega R_N}\right) + C_X} \quad (3)$$

$$VG3MX = \frac{\left(C_G \cdot (N \cdot (1 - 63G3P) - 0.5) + C_X \cdot (1 - 64G3P) + \frac{1}{3j\omega R_N} \cdot (N \cdot (1 - 64G3P) - 1)\right)}{(N-1) \cdot \left(\frac{C_G}{2} + \frac{1}{3j\omega R_N}\right)} \quad (4)$$

The analysis can be extended to N units online sharing the bus, as shown in (3). For the two-unit system in Fig. 2 ($N = 2$), the measured field data indicate a $64G3N_{RATIO}$ of 0.66 with one unit online and 0.42 with both units online.

If the zero-sequence network parameters are known, (3) can be simplified and rearranged as (4), with the assumption that the third harmonic produced by the paralleled units, $VG3_n$, is identical. This provides the worst-case $VG3_n/VG3$ ratio magnitude (VG3MX setting) that allows 64G3N to remain secure.

Actual field data from multiple installations were used to confirm the suitability of this function and to provide default setting guidance that is biased toward security while maintaining good availability when all units sharing the bus are similar.

VG3MX is plotted in Fig. 7 as a function of the number of units (N), with the following relatively stringent assumptions:

- C_X is zero. Additional capacitance at the terminals adds additional security to the scheme.
- To limit transient overvoltages, the NGR may be sized to $1/(3\omega[C_G + C_X])$. This allows compensation of the system capacitances when a single unit is online. When multiple units share the bus, as in Fig. 7, they contribute their own paralleled NGRs to the network. Another option is to size the NGRs to $1/(3\omega[C_G + C_X/N])$, which only compensates a portion of C_X when primarily considering paralleled operation. In our case, we leave a 25 percent margin and assume the worst-case resistance from the NGR (and neutral grounding transformer [NGT] leakage), which adds to $0.75 \cdot 1/(3\omega[C_G + C_X])$.
- A 10 percent margin is provided on top of the 64G3P pickup of 15 percent to accommodate other cases that impact security [4]. This implies that we do not expect $VN3$ to drop below 25 percent of $VG3$ during paralleled operation, barring other external third-harmonic events.
- We assume the worst-case angle of $VG3_n/VG3$, which depends on the zero-sequence network. For example, for the assumptions stated above and a two-unit case, the angle of $VG3_n/VG3$ evaluates to 29 degrees.

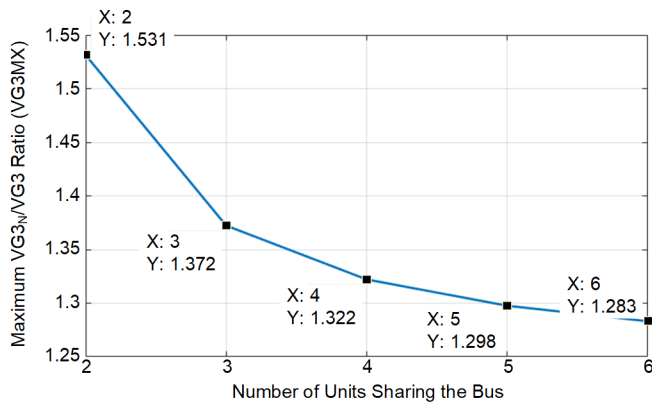


Fig. 7. Secure VG3MX setting for N units sharing a bus

Fig. 8 shows the behavior of the 64G3 element for a two-unit and a three-unit system using (3) as the maximum third-harmonic contribution from the paralleled units ($VG3N$) increases. The stringent circuit parameters considered for Fig. 7 were used.

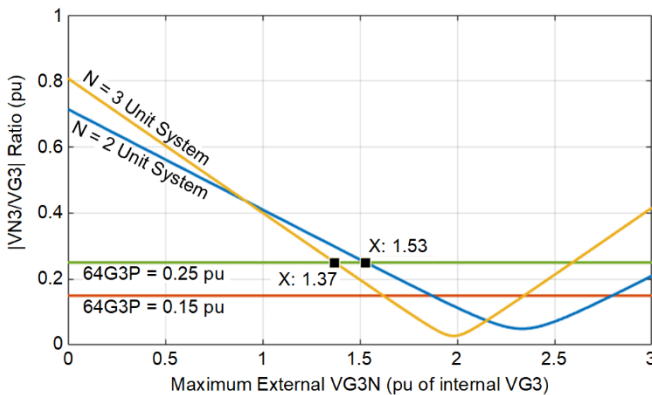


Fig. 8. 64G3 behavior as a function of maximum external $VG3N$ for a two-unit and a three-unit system considering stringent circuit parameters

The availability of this function is shown via the logic in Fig. 9. This logic allows generator owners to check whether neutral-side coverage is available for the desired operating conditions for the paralleled system. The minimum $VG3$ supervision of 0.01 pu (of V_{LN}) is inherited from 64G3, whereas 64G3NBL is obtained from 64G3N (see Fig. 6).



Fig. 9. 64G3 availability logic

It is possible for the range of $VG3$ produced by the individual generating units to be less than the $VG3MX$ evaluated using (4). In such cases, the communications scheme may be left disabled.

D. Design Validation

We evaluated the performance of the 64G3 algorithm in the Simulink model shown in Fig. 10 based on real system impedances. By using (4) with the system parameters from Table I and substituting 64G3P with 25 percent (margin of 10 percent), we obtained $VG3_n/VG3 = 1.88 \angle 31^\circ$, which corresponds to $VG3MX = 1.88$. Fig. 10 shows that the $VN3/VG3$ ratio is barely above 0.25 when the blocking signal 64G3NBL is deasserted.

TABLE I
EXAMPLE GENERATOR PARAMETERS

| Parameter | Data |
|---|--|
| Number of units | $N = 2$ |
| Nominal voltage | 13.8 kV |
| Nominal power per unit | 60 MVA |
| Neutral PT ratio | $PTRN = 13.8 \text{ kV}:230 \text{ V} = 60$ |
| Percentage of stator winding protection desired | 64G3P = 15% |
| Capacitances (per phase) | Stator ground (C_G): 0.657 μF External (C_X): 0.200 μF |
| Neutral grounding resistance (for each unit) | $R_N = 0.287 \Omega_{\text{sec}} = 1,032 \Omega_{\text{pri}}$ equal to $1/(3\omega[C_G + C_X])$ |

We also applied various internal faults for the system above. 64G3 was on the threshold of operation for the following:

- Ground faults at 15 percent of the stator winding with a fault resistance (R_F) of 0 Ω .
- Faults at the neutral with $R_F < 175 \Omega$.

The element was secure for internal faults above 15 percent and external faults at the generator terminals (regardless of R_F).

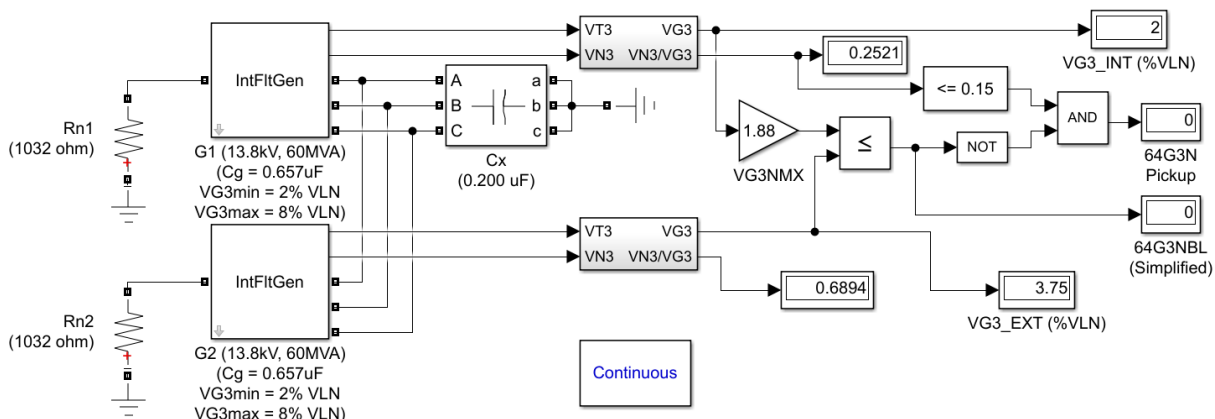


Fig. 10. Simulink model used to validate analytical results for 64G3N

E. Cross-Compound Units

For cross-compound units, each unit sharing the bus can produce widely different levels of VG3, making the availability of the approach discussed in this section very low. In such cases, the compensated differential method shown in the Appendix can be used. The application hurdle is to install a neutral PT on the LP unit, which is not commonly done. This is a great reason to use injection schemes (described in Section III, Subsection E) to obtain 100 percent stator ground protection on cross-compound units.

III. INJECTION SCHEMES

Multiple methods for applying injection schemes to stator windings have been used over the years [3] [5] [6], but the most common option is to use the existing grounding transformer to couple the injection signal to the primary circuit, as shown in Fig. 11. The corresponding circuit seen by a 64S relay is shown in Fig. 12.

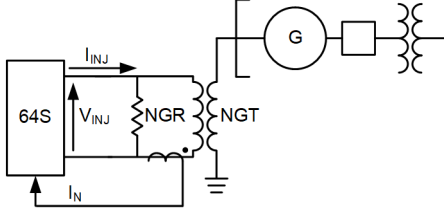


Fig. 11. Common injection scheme (64S) connection

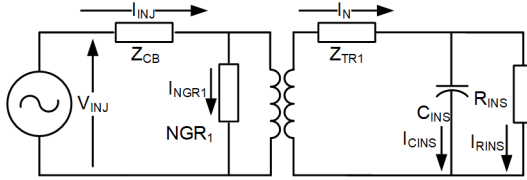


Fig. 12. Equivalent circuit for injection scheme

C_{INS} includes the phase-to-ground capacitance of the generator windings, surge arrester, delta winding of the GSU, AUX, and any other connected equipment. It ranges from $0.1 \mu\text{F}$ to several μF [7]. The NGR ohmic value is sized to compensate for C_{INS} at nominal frequency and can range from 0.1 to 3Ω secondary, or 500Ω to a few $\text{k}\Omega$ primary, depending on the value of C_{INS} . The NGT ratio typically ranges from 30 to 120.

R_{INS} is the insulation resistance and is typically much higher than the capacitive reactance. The insulation in a new generator should be well more than $100 \text{ k}\Omega$ [8].

I_N is the current that flows up the generator neutral, then through the insulation resistance (R_{INS}) and capacitance (C_{INS}).

Z_{CB} is the cable impedance from the injection source to the NGR. By design, the injection source is intended to be located close to the neutral grounding cubicle, leading to a nearly

resistive Z_{CB} of 0.1 to 0.2Ω . If it is located far away, the impedance could be on the order of 1Ω .

Z_{TR} is typically around 4 to 6 percent of the transformer's rated base. Since transformers are typically rated at 25 to 100 kVA, the resulting impedance seen from the secondary side is very small. The importance of these impedances is demonstrated later in this paper.

A. Real-World 64S Application

In this subsection, we consider the expected currents under normal and faulted conditions for a real-world application of the 60 MVA, 13.8 kV hydroelectric generator shown in Fig. 13. The generator and connected equipment have a total capacitance of $2 \mu\text{F}$, or $-j1.229 \Omega$ secondary at an 18 Hz injection frequency. The grounding transformer is a 13,800/230 V, 100 kVA unit with 4.3 percent leakage reactance. The NGR is 0.28Ω and Z_{CB} is 0.64Ω secondary. A constant injected current (I_{INJ}) magnitude of 2.5 A is used in the calculations.

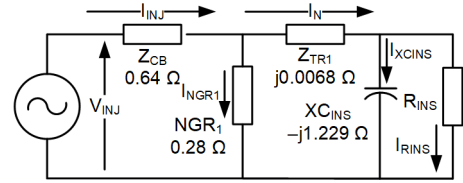


Fig. 13. Equivalent circuit for real-world 64S application in secondary ohms

As the stator winding insulation begins to break down, leading to a fault, the value of R_{INS} decreases from the typical values for a healthy stator winding. Table II shows the changes in the circuit currents and voltages as the value of R_{INS} decreases. The insulation capacitance and resistance values are calculated using the measured voltages and currents shown.

For insulation resistances above $10 \text{ k}\Omega$, large changes in R_{INS} result in minute changes in most of the measured quantities, especially I_N , which is used to extract the insulation resistance measurement. Therefore, considering typical measurement errors associated with the relays and CTs used, the accuracy of the measurement is limited. This is acceptable because the 64S relay is intended to detect ground faults where the insulation resistance is lower. Common trip and alarm thresholds range from 1 to $10 \text{ k}\Omega$ [7].

This resolution and the insulation resistance reported by the 64S relay during normal operating conditions often surprises those who analyze insulation resistance test measurements, which are typically hundreds of megaohms to gigaohms. The high values are due to the fact that insulation resistance testing is done with the stator windings isolated from ground with dc test voltages ranging from 1 to 10 kV. In contrast, the 64S relay performs the measurement during normal operating conditions with insulation capacitances in the circuit and ac voltages in the range of 50 to 100 V primary induced through the NGT.

TABLE II
CALCULATED CIRCUIT PARAMETERS FOR UNIT-CONNECTED OPERATION WITH VARYING R_{INS}

| R_{INS} (k Ω primary) | V_{INJ} (V secondary) | I_{NGR} (A secondary) | I_N (A secondary) | Calculated Insulation Capacitance (μ F primary) | Calculated Insulation Resistance (k Ω primary) |
|-----------------------------------|----------------------------|----------------------------|------------------------|---|--|
| 100 | $2.26\angle-3.8^\circ$ | $2.41\angle-12.8^\circ$ | $0.55\angle74.7^\circ$ | 2.0 | 100 |
| 50 | $2.26\angle-3.7^\circ$ | $2.39\angle-12.7^\circ$ | $0.55\angle72.3^\circ$ | 2.0 | 50 |
| 25 | $2.25\angle-3.6^\circ$ | $2.35\angle-12.4^\circ$ | $0.55\angle67.5^\circ$ | 2.0 | 25 |
| 10 | $2.21\angle-3.3^\circ$ | $2.22\angle-11.7^\circ$ | $0.56\angle54.3^\circ$ | 2.0 | 10 |
| 5 | $2.16\angle-2.8^\circ$ | $2.04\angle-10.7^\circ$ | $0.62\angle37.5^\circ$ | 2.0 | 5 |
| 2 | $2.05\angle-1.9^\circ$ | $1.64\angle-8.4^\circ$ | $0.91\angle15.2^\circ$ | 2.0 | 2 |
| 1 | $1.94\angle-1.0^\circ$ | $1.23\angle-5.8^\circ$ | $1.28\angle5.6^\circ$ | 2.0 | 1 |
| 0.5 | $1.83\angle-0.3^\circ$ | $0.82\angle-2.4^\circ$ | $1.68\angle1.2^\circ$ | 2.0 | 0.5 |
| 0.25 | $1.74\angle0.2^\circ$ | $0.50\angle1.9^\circ$ | $2.00\angle-0.5^\circ$ | 2.0 | 0.25 |

TABLE III
CALCULATED CIRCUIT PARAMETERS DURING PARALLELED OPERATION

| R_{INS} (k Ω primary) | V_{INJ} (V secondary) | I_{NGR} (A secondary) | I_N (A secondary) | Calculated Insulation Capacitance (μ F primary) | Calculated Insulation Resistance (k Ω primary) |
|-----------------------------------|----------------------------|----------------------------|------------------------|---|--|
| 100 | $1.93\angle-1.9^\circ$ | $1.21\angle-10.6^\circ$ | $1.33\angle9.6^\circ$ | 3.52 | 0.998 |
| 50 | $1.93\angle-1.8^\circ$ | $1.21\angle-10.5^\circ$ | $1.33\angle9.5^\circ$ | 3.52 | 0.989 |
| 25 | $1.93\angle-1.8^\circ$ | $1.19\angle-10.4^\circ$ | $1.34\angle9.2^\circ$ | 3.52 | 0.969 |
| 10 | $1.92\angle-1.7^\circ$ | $1.16\angle-10.0^\circ$ | $1.37\angle8.5^\circ$ | 3.52 | 0.916 |
| 5 | $1.91\angle-1.5^\circ$ | $1.11\angle-9.4^\circ$ | $1.42\angle7.4^\circ$ | 3.52 | 0.839 |
| 2 | $1.87\angle-1.1^\circ$ | $0.98\angle-7.8^\circ$ | $1.54\angle5.0^\circ$ | 3.52 | 0.670 |
| 1 | $1.83\angle-0.7^\circ$ | $0.82\angle-5.7^\circ$ | $1.69\angle2.8^\circ$ | 3.52 | 0.502 |
| 0.5 | $1.77\angle-0.2^\circ$ | $0.62\angle-2.5^\circ$ | $1.89\angle0.8^\circ$ | 3.52 | 0.334 |
| 0.25 | $1.72\angle0.1^\circ$ | $0.41\angle2.1^\circ$ | $2.09\angle-0.4^\circ$ | 3.52 | 0.200 |

B. 64S Measurements for Paralleled Units

The sensitivity of this scheme when applied to the configuration in Fig. 1 can be compared with the data from the previous subsection as a benchmark for a unit-connected machine. Fig. 14 shows the single-line diagram and equivalent circuit from Fig. 13 modified (in red and dashed) to include an identical generator connected in parallel. X_{CINS} includes the capacitance of both units, the bus, and the transformer delta windings. Similarly, only one insulation resistance is shown.

Table III shows the resulting measurements and calculated values from the circuit of Fig. 14. While Table III shows that there are still variations in the currents and voltages measured, the variation from the maximum to the minimum value for each quantity is significantly less when generators are operated in parallel. As the final two columns indicate, the calculated insulation capacitance and resistance have significant errors. The capacitance should be 3.73 μ F. However, the largest error appears in the insulation resistance measurement, which is always reported to be below 1 k Ω (value of NGR_2). Therefore, the trip pickup would need to be set below 1 k Ω with some margin. A setting of 0.5 k Ω would be reasonable from a security perspective, but the relay would not detect a fault with more

than approximately 1 k Ω of fault resistance. This number could vary depending on the relay and CT accuracy. Regardless, the sensitivity of this scheme for fault detection is approximately ten times less than that of the unit-connected configuration.

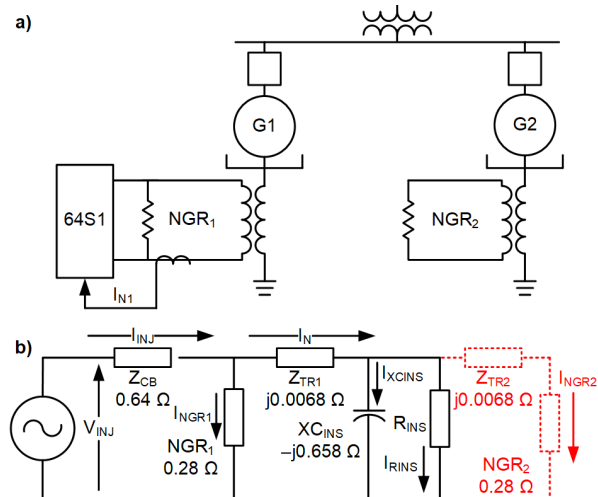


Fig. 14. Injection scheme applied to paralleled generators: a) single-line diagram and b) equivalent circuit

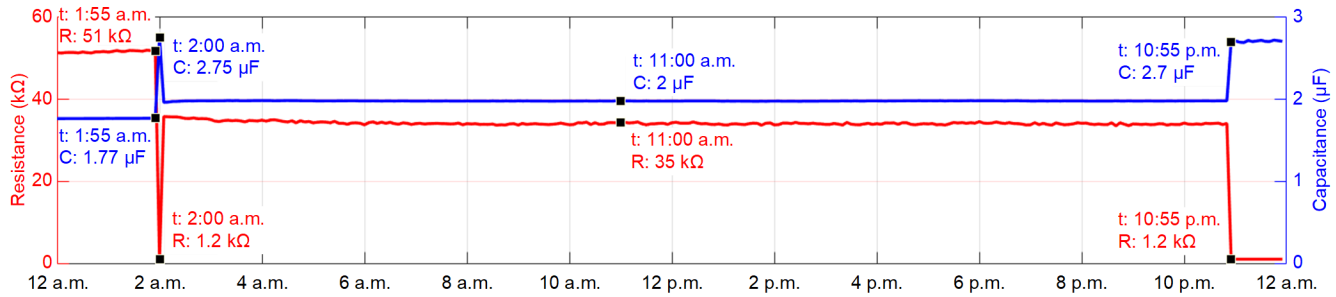


Fig. 15. Stator insulation resistance and capacitance measured for a field event during a 24-hour period

TABLE IV
CALCULATED CIRCUIT PARAMETERS DURING PARALLELED OPERATION WITH DIFFERENTIAL CT CONFIGURATION

| R_{INS} (kΩ primary) | V_{INJ} (V secondary) | I_{NGR} (A secondary) | $I_N - I_{NGR2}$ (A secondary) | Calculated Insulation Capacitance (μF primary) | Calculated Insulation Resistance (kΩ primary) |
|---------------------------|----------------------------|----------------------------|-----------------------------------|---|--|
| 100 | $1.93 \angle -1.9^\circ$ | $1.21 \angle -10.6^\circ$ | $0.52 \angle 76.6^\circ$ | 3.72 | 49.50 |
| 50 | $1.93 \angle -1.8^\circ$ | $1.21 \angle -10.5^\circ$ | $0.52 \angle 75.3^\circ$ | 3.72 | 33.12 |
| 25 | $1.93 \angle -1.8^\circ$ | $1.19 \angle -10.4^\circ$ | $0.51 \angle 72.7^\circ$ | 3.72 | 19.93 |
| 10 | $1.92 \angle -1.7^\circ$ | $1.16 \angle -10.0^\circ$ | $0.51 \angle 65.1^\circ$ | 3.70 | 9.08 |
| 5 | $1.91 \angle -1.5^\circ$ | $1.11 \angle -9.4^\circ$ | $0.53 \angle 53.5^\circ$ | 3.68 | 4.76 |
| 2 | $1.87 \angle -1.1^\circ$ | $0.98 \angle -7.8^\circ$ | $0.65 \angle 30.2^\circ$ | 3.62 | 1.96 |
| 1 | $1.83 \angle -0.7^\circ$ | $0.82 \angle -5.7^\circ$ | $0.90 \angle 14.3^\circ$ | 3.51 | 0.99 |
| 0.5 | $1.77 \angle -0.2^\circ$ | $0.62 \angle -2.5^\circ$ | $1.28 \angle 5.2^\circ$ | 3.30 | 0.50 |
| 0.25 | $1.72 \angle 0.1^\circ$ | $0.41 \angle 2.1^\circ$ | $1.68 \angle 1.1^\circ$ | 2.87 | 0.25 |

Fig. 15 shows the insulation resistance and capacitance measured over a 24-hour period in 5-minute intervals from a real-world installation. The generator with the 64S relay (G1) was offline and de-energized until 2 a.m. The relay measured a R_{INS} of 52 kΩ and a C_{INS} of 1.77 μF. At 2 a.m., the generator without the 64S relay (G2) was online. At this time, G1 was synchronized and the two generators were paralleled for less than 10 minutes, resulting in a steep drop of R_{INS} to 1.2 kΩ with a C_{INS} of 2.75 μF. At 2:10 a.m., G2 was taken offline while G1 remained unit-connected to the system, resulting in a measured R_{INS} of 35 kΩ and a C_{INS} of 2 μF. This configuration was maintained until 11 p.m., when G2 was brought online and paralleled once again.

C. 64S Measurements With Differentially Connected CTs

To eliminate the large measurement error, the current flowing through the parallel generator ground must be considered in the current measurement. By wiring a second CT in parallel, a differential current can be measured, effectively removing the undesired component. This configuration is shown in Fig. 16. The second injection scheme (64S2) is discussed in Section IV, Subsection D.

Applying this configuration to the circuit from Fig. 14, the correct insulation current is $I_N - I_{NGR2}$. Table IV shows the results from Table III with this updated quantity and the resulting calculated insulation capacitance and resistance values.

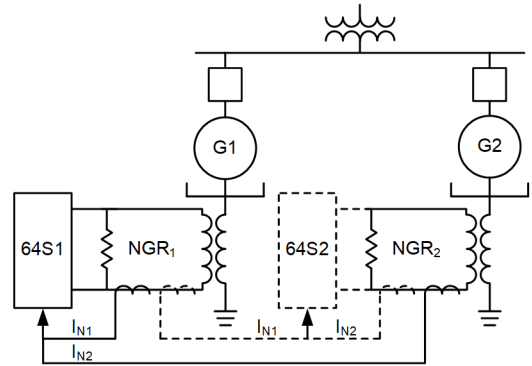


Fig. 16. 64S configuration for parallel generators with differentially connected CTs

The results in Table IV show significant improvements in the measured quantities, especially for large values of R_{INS} . For values of R_{INS} greater than 10 kΩ, the insulation capacitance is very close to the actual value of 3.73 μF. The insulation resistance is at least 50 percent of the actual value, with the accuracy improving as R_{INS} decreases. With this improvement, the relay could be configured to alarm at 10 kΩ and trip for a 2 kΩ fault with reasonably good accuracy.

The relay measures and stores the value of Z_{TR1} during the commissioning procedure. Using this stored value, the relay calculates the circuit insulation impedance (Z_{INS}) using (5).

$$Z_{INS} = \frac{V_{NGR1} - (I_N - I_{NGR2}) \cdot Z_{TR1}}{I_N - I_{NGR2}} \quad (5)$$

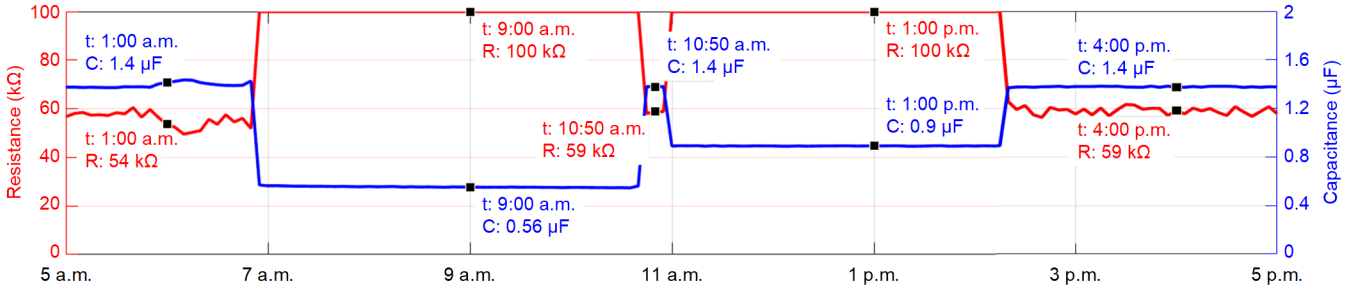


Fig. 17. Stator insulation resistance and capacitance measured with differentially connected CTs for a field event

Combining the current measurements externally results in the correct removal of I_{NGR2} from the denominator but an incorrect removal from the numerator. Hence, large values of R_{INS} result in a larger error, which is not a significant issue because the trip and alarm thresholds are set much lower. Trending these measurements on healthy machines, however, could create some confusion.

Fig. 17 shows a real-world event from a generating station with two paralleled units. The calculated insulation resistance and capacitance demonstrate the performance of the corrected method using differentially connected CTs. From 5 a.m. to 6:50 a.m., the two units operated in parallel. From 6:50 a.m. to 10:35 a.m., G1 was offline and de-energized. The units were again paralleled from 10:45 a.m. until 11:00 a.m., at which time the other generator was taken offline, and the generator with the 64S relay operated in a unit-connected configuration. This configuration was maintained until 2:20 p.m., when the generators were paralleled once more.

Although satisfactory performance can be achieved using differentially connected CTs, an improvement to this scheme can be made by measuring the CT outputs individually. If I_N and I_{NGR2} are measured individually, (5) can be modified into (6).

$$Z_{INS} = \frac{V_{NGR1} - I_N \cdot Z_{TR1}}{I_N - I_{NGR2}} \quad (6)$$

The resulting R_{INS} and C_{INS} values, by considering the real and imaginary parts of Z_{INS} , match expected values across the entire range of R_{INS} values shown in Table II, Table III, and Table IV.

D. Injection Scheme Requirements for Paralleled Units

If an injection scheme is only applied to the relay of G1 of Fig. 14a, protection is unavailable to G2 if the breaker corresponding to either generator is open. This is an important reason to equip each unit with its own injection scheme as shown in Fig. 16.

Furthermore, when using multiple injection sources, it is necessary to use different injection frequencies; otherwise, it is impossible to distinguish which injection source produces the current measured at the NGR of the paralleled unit. The situation is identical to the problem explained in Section II, Subsection A, in which the generator acts as the injection source and produces a single (third-harmonic) frequency. Injection schemes that use different frequencies are available today [3].

E. Application to Cross-Compound Units

A third-harmonic scheme can be applied to the HP unit shown in Fig. 18 but not the LP unit. This is due to the unavailability of a third-harmonic measurement at the LP neutral. While it is feasible to add a PT to the LP neutral, it is simpler to apply a subharmonic injection scheme to the HP unit, as shown in Fig. 18.

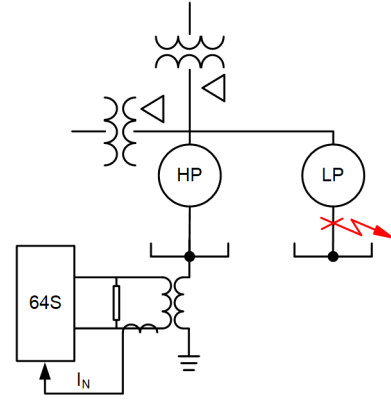


Fig. 18. Injection scheme applied to a cross-compound generator

The scheme is equivalent to that of Fig. 16 but without the need to measure current at the LP neutral. Complete coverage for both units is provided.

IV. SELECTIVITY

The previous sections presented two approaches that help provide 100 percent stator ground protection when multiple units share a common bus. This section answers the question “Which breaker do we trip if we have securely determined that a ground fault exists?”

The main problem is that the fundamental voltages used for protecting all units sharing the common bus look identical during a ground fault. This is because the impedance of a generator winding is negligible in comparison to the neutral resistance and shunt capacitive reactance. Furthermore, the ground fault current for high-impedance grounded units is very small (typically beyond the detection limits of conventional CTs), which makes it difficult to measure. Consequently, the most common approach used today is to trip a predetermined trip of the other units one-by-one until the fault is no longer detected. While a valid approach, it will more often than not result in a loss of more generation than required. In some cases,

the fire suppression system, which triggers the release of CO₂ during lockout trips (such as a ground fault), cannot handle simultaneous trips on multiple units. In contrast, tripping selectively causes minimal disruption to the generation and the system.

In this section, we introduce two approaches to identify the faulted unit. Neither method trips the breaker on its own. The existing ground fault protection elements provide a reliable indication that a fault has occurred, after which the selectivity scheme identifies the faulted unit. The selectivity scheme leverages the existing staggered trip logic by biasing the staggered trip process; instead of tripping a predetermined unit, the scheme identifies the unit most likely to be faulted to trip first. If the faulted machine cannot be identified, the logic falls back to the conventional staggered trip sequence.

A. Third-Harmonic and Fundamental Voltage Differential (87V31)

Consider the single-line diagram and the equivalent fundamental and third-harmonic faulted circuits shown in Fig. 19.

The third-harmonic scheme leverages differences in the third-harmonic voltage distributions in the faulted and unfaulted units when there is a circulating component between them. This approach is illustrated in Table V, Table VI, and Table VII. We placed metallic faults at various locations m of G1 in Fig. 19 and recorded the ratios of the fundamental neutral voltage divided by the positive-sequence voltage ($VN/V1$) and $VN3/VG3$.

In Table V, $VG3_{G1}$ is 1 pu, whereas $VG3_{G2}$ is 1.25 pu. The VG3s for the two generators are assumed to be in phase for this analysis. It is evident that the ratios are in agreement on the faulted machine (G1) but not on the unfaulted machine (G2) except right at the terminal.

In Table VI, $VG3_{G1}$ is 1 pu, whereas $VG3_{G2}$ is 0.8 pu. The ratio discrepancy once again occurs on the unfaulted machine. In Table VII, VG3 is 1 pu for both machines. The ratios agree on both machines because there is no third-harmonic circulation between the units.

$VN/V1$ for both units always sees the same voltages. $VN3/VG3$ of the faulted unit sees the same ratio as $VN/V1$. For the unfaulted units, a different ratio is observed. For example, in Row 2 of Table VI, the absolute difference for the faulted unit is $|VN3/VG3 - VN/V1| = |0.15 - 0.15| = 0$. The absolute difference for the unfaulted unit is $|-0.06 - 0.15| = 0.21$. This method provides selectivity for faults close to the neutral and is blind to faults at the terminals.

While $VN/V1$ ranges from 0 to 1, $VN3/VG3$ can be larger. However, to use the biased staggered tripping process detailed in Section IV, Subsection C, we limit the maximum value of $VN3/VG3$ to 1. Finally, we invert the signal for the sake of convention, as shown in (7), such that a higher differential signal (87V31) indicates the faulted unit.

$$87V31 = 1 - \min\left(\left|\frac{VN3}{VG3} - \frac{VN}{V1}\right|, 1\right) \quad (7)$$

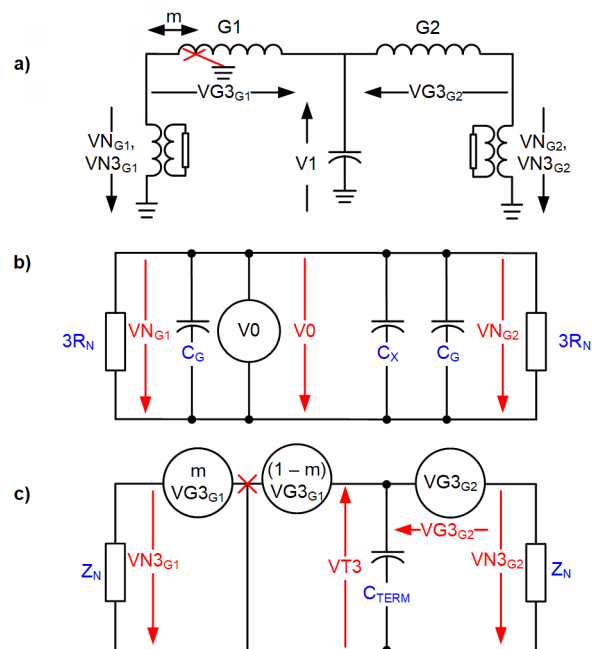


Fig. 19. a) Single-line diagram b) fundamental circuit, and c) third-harmonic circuit

TABLE V
VG3_{G1} = 1.00 AND VG3_{G2} = 1.25 (MISMATCH = +0.25)

| m | G1 | | G2 | |
|------|-------|---------|-------|---------|
| | VN/V1 | VN3/VG3 | VN/V1 | VN3/VG3 |
| 0.0 | 0.0 | 0 | 0 | 0.2 |
| 0.15 | 0.15 | 0.15 | 0.15 | 0.32 |
| 0.5 | 0.5 | 0.5 | 0.5 | 0.6 |
| 1.0 | 1.0 | 1.0 | 1.0 | 1.0 |

TABLE VI
VG3_{G1} = 1.00 AND VG3_{G2} = 0.80 (MISMATCH = -0.20)

| m | G1 | | G2 | |
|------|-------|---------|-------|---------|
| | VN/V1 | VN3/VG3 | VN/V1 | VN3/VG3 |
| 0.0 | 0.0 | 0 | 0 | -0.25 |
| 0.15 | 0.15 | 0.15 | 0.15 | -0.06 |
| 0.5 | 0.5 | 0.5 | 0.5 | 0.38 |
| 1.0 | 1.0 | 1.0 | 1.0 | 1.0 |

TABLE VII
VG3_{G1} = 1.00 AND VG3_{G2} = 1.00 (MISMATCH = 0.00)

| m | G1 | | G2 | |
|------|-------|---------|-------|---------|
| | VN/V1 | VN3/VG3 | VN/V1 | VN3/VG3 |
| 0.0 | 0.0 | 0 | 0 | 0.0 |
| 0.15 | 0.15 | 0.15 | 0.15 | 0.15 |
| 0.5 | 0.5 | 0.5 | 0.5 | 0.5 |
| 1.0 | 1.0 | 1.0 | 1.0 | 1 |

87V31 ranges from 0 for the unit that is least likely to be faulted to 1 for the unit with an internal metallic fault. This method was validated using the model shown in Fig. 10.

B. Sensitive Directional Element (32S)

IEEE C37.102 [9] shows a directional overcurrent element (67N in Fig. 20) applied to a high-impedance grounded generator. Core-balance CTs are used at the terminals to minimize measurement errors and implement the 67N function, which largely limits the applicability of this function to machines with phase leads small enough to pass through a single core-balance CT.

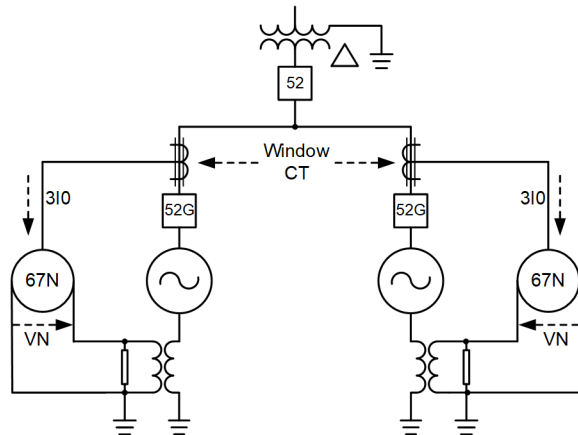


Fig. 20. Directional overcurrent scheme with core-balance CTs [9]

Modern relays are often equipped with sensitive current inputs. Instead of current inputs rated at 5 A or 1 A, the inputs can be rated at 0.2 A. Based on lab tests, such inputs can detect 1 mA of current with an error of 2.5 percent. This subsection describes the implementation of a sensitive directional element (32S) with flexible instrument transformer requirements.

1) Theory of Operation

The incremental zero-sequence circuit for a faulted circuit of Fig. 20 is shown in Fig. 21. The V0 voltage sources represent the location of the ground fault. Only one V0 source is active at a time, representing a single ground fault at the stator terminals. A fault closer to the neutral results in a smaller V0 magnitude.

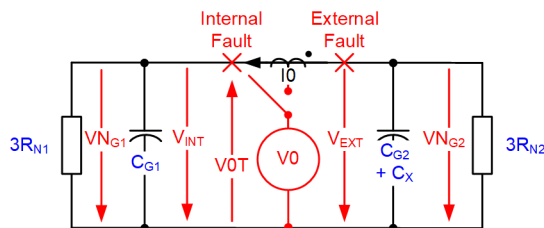


Fig. 21. Zero-sequence circuit during an external or internal fault, depending on position of the fault switch

For an external (reverse) fault, the protected unit sources a charging current from its stator ground insulation capacitance (C_{G1}) and the grounding resistance ($3R_{N1}$). The zero-sequence admittance (Y_{REV}) measured by a relay in Fig. 21 that uses the neutral voltage (VN) and residual currents (I0) is calculated as shown in (8):

$$Y_{REV} = -\left(j\omega C_{G1} + \frac{1}{3R_{N1}} \right) \quad (8)$$

For an internal (forward) fault, the external zero-sequence network, C_X , C_{G2} , and R_{N2} discharge through the CT at the generator terminal, resulting in the admittance measurement (Y_{FWD}) shown in (9):

$$Y_{FWD} = +\left(j\omega(C_{G2} + C_X) + \frac{1}{3R_{N2}} \right) \quad (9)$$

For high-impedance grounded generators, because the NGR is sized to match the system capacitance, the current leads the voltage by 45 degrees for a forward fault and leads by 225 degrees ($45 + 180$) for a reverse fault. The admittance method has been used to provide sensitive detection of ground faults in compensated systems [10] [11].

2) Instrument Transformer Requirements

The polarizing signal can be measured by the wye-grounded, broken-delta, or neutral voltage from the NGT. Since a neutral voltage is practically necessary for ground fault detection, we use the neutral voltage (VN) as the polarizing signal. This approach has been suggested in IEEE C37.102 (see Fig. 20) [9].

Any terminal CTs that measure zero-sequence current and provide it to the relay are acceptable. For core-balance CTs, the CT errors are very small. However, these CTs are only available on the smallest units. The errors depend on the CT ratio and are likely to be less than 1 mA.

Using residually connected phase CTs to measure 310 is the most common configuration. The errors are larger than in the previous applications, possibly tens of milliamperes. The steady-state standing error could be larger than the ground fault current to be detected!

3) Element Design and Security

To allow for flexible CT requirements, such as a residually connected phase CTs, a short memory (TMEM) can remove pre-fault measurement errors to provide an incremental residual current, DI_{sens}, as shown in (10).

$$DI_{sens} = Isens_k - Isens_{k-TMEM} \quad (10)$$

Y0SENS, calculated in (11), is scaled to primary units to allow comparison with the forward (Y0FTH) and reverse (Y0RTH) thresholds set to +0.1 mS and -0.1 mS primary (Fig. 22), allowing the element to respond to primary zero-sequence impedances lower than 10 kΩ.

$$Y0SENS = \text{Re} \left(\frac{DI_{sens} \cdot e^{-j\frac{\pi}{4}}}{3 \cdot VN} \right) \cdot \frac{CTR}{PTRN} \quad (11)$$

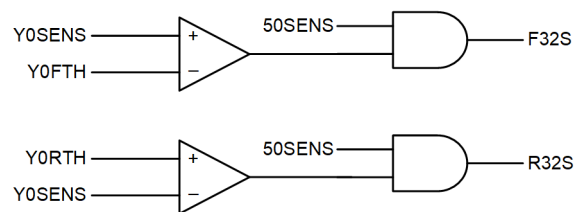


Fig. 22. Raw directional element comparison

F32S and R32S are supervised by an overcurrent element operating (Fig. 23) on DI_{sens} set to 4 mA (2 percent of the 0.2 A current input).

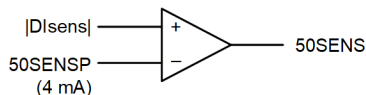


Fig. 23. Sensitive overcurrent supervision

The directional element has a short pickup timer (e.g., 1 to 2 cycles), after which it provides a forward (F32ST) or reverse (R32ST) declaration, as shown in Fig. 24. These indications stay latched for the entire duration that the element is enabled via 32SEN (e.g., 5 seconds).

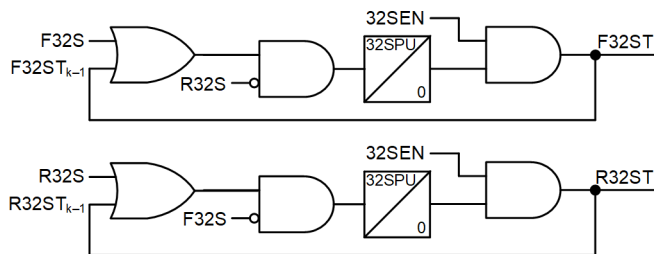


Fig. 24. Secure latched directional element declaration

The element is guarded by the one-shot arming logic shown in Fig. 25. The element arms the logic once the system is healthy for a 32SARM duration (e.g., 10 seconds) with $V_1 > 85\%$ and $V_N < 2.5\%$. This indication does not drop out for 64GARST (e.g., 5 seconds).

The 32S element enables (32SEN) for the duration specified by 64GARST if a ground condition is detected ($V_N > 5\%$). 32SEN does not assert for GSU high-voltage events that couple via the GSU interwinding capacitance due to supervision by an impedance-based negative-sequence directional element (32Q).

The 32S element avoids a misdeclaration of the direction during intermittent faults by using a dropout timer (64GARST) that qualifies 32SEN. The algorithm is only run once at fault inception (32SONE), and it opens a short window to determine the fault direction (F32ST or R32ST). The directional declaration is sealed in for 64GARST (e.g., 5 seconds) facilitating detection of the intermittent fault direction. The security features of 32S allows the direction to be provided only when there is a clear indication. Otherwise, the logic is not run and/or directionality is not provided.

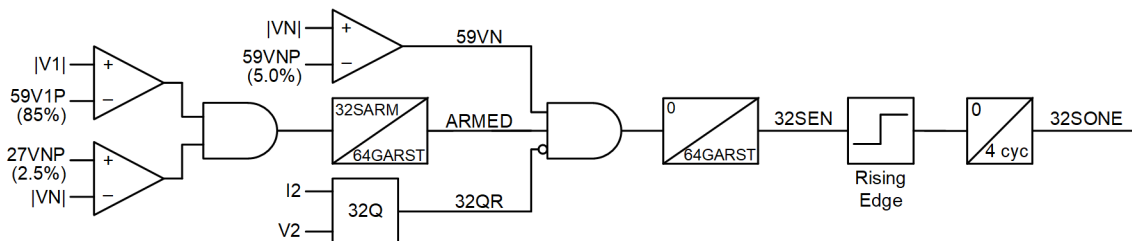


Fig. 25. Secure one-shot arming logic used by 32S to facilitate detection of intermittent fault direction

4) Element Applicability and Sensitivity

The primary sensitivity limit for this element is the minimum incremental current of 4 mA. This prevents the detection of faults at the bottom m percent of the winding, as shown in (12), where Y_0 corresponds to Y_{FWD} in (9).

$$m = \frac{0.004 \cdot \text{CTR}}{\sqrt{3} \cdot V_{\text{nomLL}} \cdot |Y_0|} \cdot 100\% \quad (12)$$

We inserted the system parameters of Table VIII into (12) and (9) to yield (13) and (14), respectively.

TABLE VIII
EXAMPLE SYSTEM PARAMETERS USED FOR 32S

| Parameter | Data |
|--|--|
| Number of units | $N = 2$ |
| Nominal voltage | 13.8 kV |
| Nominal power per unit | 24 MVA |
| CT | $\text{CTR} = 1500:5 = 300$ |
| PT ratio | $\text{PTR} = 13800:115$ |
| Neutral PT ratio | $\text{PTRN} = 13800:230$ |
| Capacitances (per phase) | Stator ground (C_G): 0.342 μF External (C_X): 0.100 μF GSU interwinding (C_{IW}): 8 nF |
| Neutral grounding resistance (for each unit) | $R_N = 2,000 \Omega_{\text{pri}}$ equal to $1/(3\omega[C_G + C_X])$ |

$$m = \frac{0.004 \cdot 300}{\sqrt{3} \cdot 13,800 \cdot |Y_0|} \cdot 100\% = 21.3\% \quad (13)$$

$$Y_0 = -\left(j\omega(C_{G2} + C_X) + \frac{1}{3R_{N2}} \right) = -(0.236 \text{ mS} \angle 45^\circ) \quad (14)$$

Based on (13), the element cannot detect metallic faults at the bottom 21.3 percent of the stator winding (i.e., the element *can* detect metallic faults on the upper 78.7 percent of the stator winding).

To check the availability of this element, we applied (13) to each of the 73 high-impedance grounded generators on shared buses at the utility mentioned in Section I. The generators are rated from 0.8 to 174 MVA with CT ratios ranging from 60 to 1,600. All reverse faults were detected. For forward faults, the upper stator winding coverage was at least 67 percent, at most 99 percent, and 93 percent on average.

5) Design Validation

The model of the system shown in Fig. 26 was used in a real-time digital simulator (RTDS) with the parameters of Table VIII to verify the behavior of the faulted and unfaulted units for various conditions. We made the following observations:

- For G1 ground faults at 10, 20, 25, 50, and 100 percent of the stator winding, the relay protecting G1 declared forward for all faults above 25 percent with no declaration otherwise. The relay protecting G2 declared reverse for all faults above 25 percent, with no declaration otherwise.
- System ground faults can impose a VN that couples back through the GSU interwinding capacitance. In these cases, 32QR asserted, preventing the element from enabling (32SEN). For paralleled operation, the element did not assert.
- The element performed well even with standing CT errors. A measurement error is expected when using residually connected CTs. We added up to 100 mA of CT error and observed no degradation in the performance of the DISens calculation.
- The algorithm was resilient against frequency excursions, and the short window memory was stable.
- The algorithm was robust against circuit unbalances, such as phase-to-ground capacitance values.

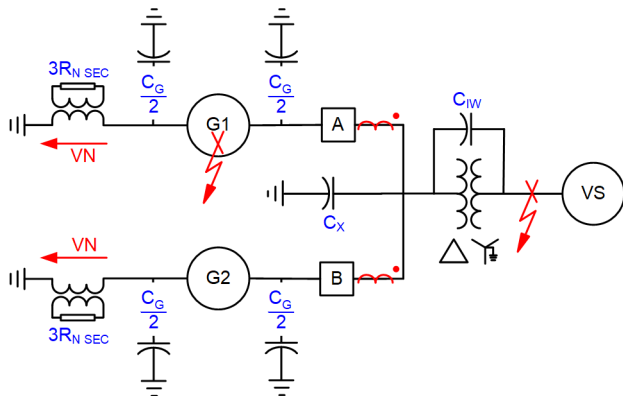


Fig. 26. System model used to validate the 32S element

The behavior of the relays protecting the faulted unit (Fig. 27) and unfaulted unit (Fig. 28) is shown for a ground fault at 25 percent of the stator winding with 10 mA error in the Isens current input. The DISens calculation is performed for the duration of the 32SONE assertion. The pre-fault current is removed correctly, as observed when compared with an event without a standing pre-fault error.

When applying a system ground fault at the terminals of the GSU high-voltage winding, the relay measures a VN of 4.2 percent, which is below the 59VNP threshold. To demonstrate the additional security provided by 32QR, we tested the operation with one unit offline, resulting in a VN of 7.7 percent, as shown in Fig. 29.

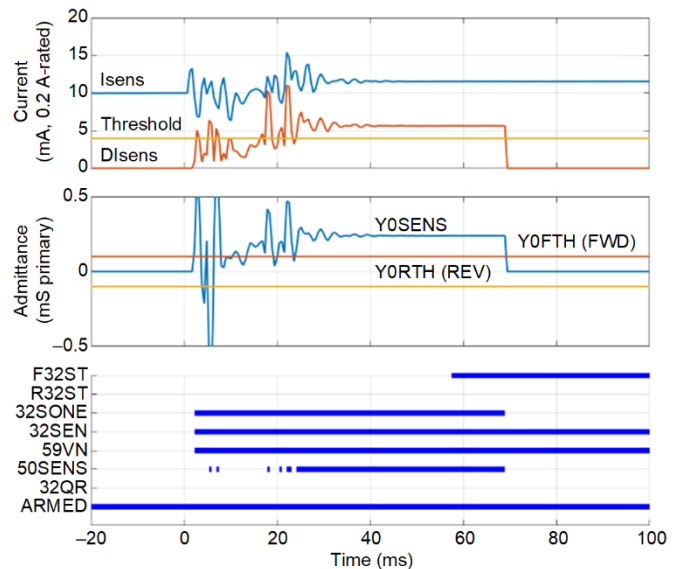


Fig. 27. Forward declaration by the relay protecting the faulted unit (G1)

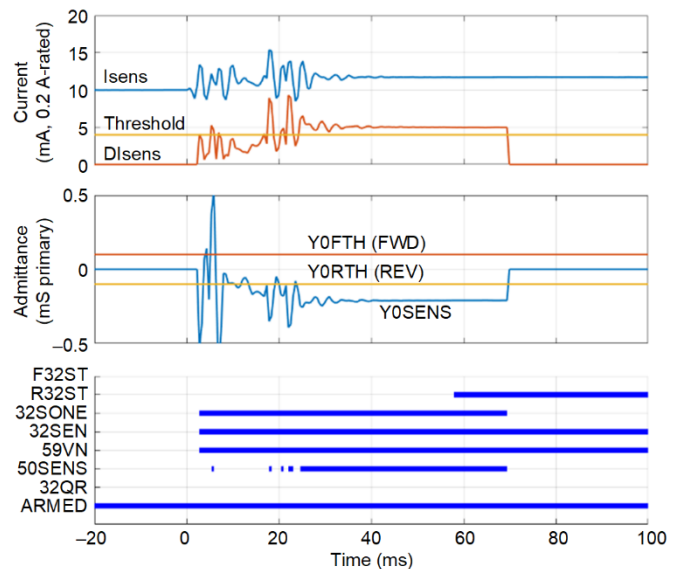


Fig. 28. Reverse declaration by the relay protecting the unfaulted unit (G2)

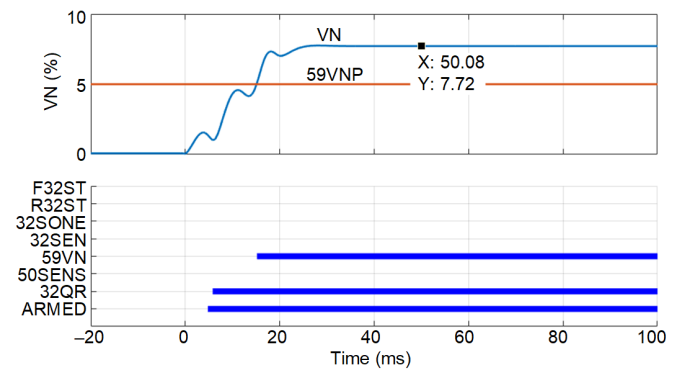


Fig. 29. Security for ground fault at GSU high-voltage terminals

When multiple units are paralleled, the zero-sequence impedance on the GSU low-voltage side is small, resulting in a small VN. However, the element must be secured for cases where the units are not paralleled or when the network impedances are unfavorable, such as when there is an extremely high GSU interwinding capacitance.

For the biased staggered tripping scheme shown in the next section, a forward declaration (F32ST) is 1, a reverse declaration (R32ST) is 0, and no declaration (default) is 0.5.

C. Biased Staggered Tripping

The conventional staggered tripping process is shown using the four-unit example in Fig. 30. Each unit is given a rank arbitrarily. Unit A trips first, followed by Unit B, Unit C, and Unit D, after intentional delays. The method is selective if the fault is on Unit A because the subsequent breakers do not trip after the ground fault clears.

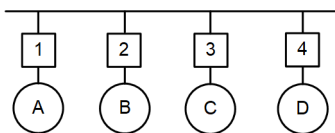


Fig. 30. Conventional staggered tripping scheme

The biased staggered trip method simply uses the selectivity methods (32S and/or 87V31) to reorder the sequence of the units tripped based on which unit is most likely to be faulted. The method requires communicating a single analog quantity to all units sharing the bus and, in the worst case (e.g., during a communications failure), behaves similarly to the conventional staggered tripping method.

Fig. 31 demonstrates the biased staggered tripping scheme. The numbers on the sides of the various units correspond to the bias factor from a selectivity scheme. A forward declaration (F32ST) is 1, a reverse declaration (R32ST) is 0, and no declaration (unknown) is 0.5. The order of the biased staggered trip starts with Unit B because it has the highest value (1). Since both Unit A and Unit D have the same value (0.5), the default rank is obeyed and Unit A trips second, followed by Unit D. Unit C trips last.

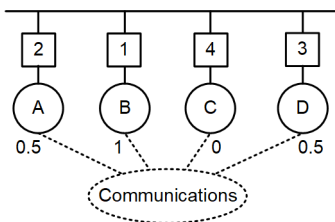


Fig. 31. Biased staggered tripping scheme

If both 32S and 87V31 are applied, they complement each other to provide a bias factor to the staggered trip. The analog value transmitted to the other relays is calculated as in (15) to ensure that there is no overlap between the cases, and 87V31 biases the indication provided by 32S.

$$\text{BIAS} = \frac{2}{3} \cdot 32S + \frac{1}{3} \cdot 87V31 \quad (15)$$

For example, for a metallic fault right at the neutral of Unit B of Fig. 32, 32S is 0.5 due to insensitivity to neutral-side faults.

But, 87V31 equals 1 for the faulted unit and something else for the unfaulted units, yielding an overall range of 0.33 to 0.66 per (15). The order of biased staggered trip is Unit B, Unit A, Unit D, then Unit C. On the other hand, if the fault was at the terminal, 87V31 would be insensitive whereas 32S would provide the desired selectivity.

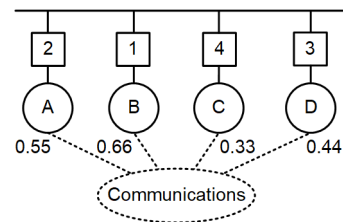


Fig. 32. Biased staggered tripping scheme with 32S and 87V31

To retain scheme simplicity in the event of a communications failure, the scheme reverts gracefully to the predetermined order defined by the conventional staggered tripping scheme.

V. CONCLUSION

Large generators, which are most often high-impedance grounded, require 100 percent stator ground protection. However, many such generators share a common bus and cannot achieve this using traditional methods. In this paper, we enhance the two approaches that have been used to protect unit-connected generators to facilitate 100 percent ground fault protection for units sharing a bus.

Third-harmonic schemes can run into issues caused by circulating third harmonics from paralleled units and by a terminal-side impedance change. We use a communications scheme to obtain information from the paralleled units to address this problem.

Injection schemes cannot be applied sensitively due to grounding sources sharing a common bus. Measuring currents from the paralleled units enhances scheme sensitivity. When applying multiple injection scheme relays to protect paralleled units, it is necessary to use relays that inject different frequencies to avoid a misoperation. Such relays are available today.

After a ground fault has been detected, the subsequent problem is to determine the faulted unit. We discuss two options that provide selectivity.

First, for a unit with a metallic fault, the operating equations corresponding to the third-harmonic scheme and a neutral overvoltage scheme normalized with the positive-sequence voltage provide the same ratio. We exploit this phenomenon to provide selectivity.

Second, modern relays are often equipped with sensitive current inputs. We use the sensitive current input to measure the zero-sequence current from the network capacitance and grounding resistances to distinguish internal and external faults. Based on system data from 73 high-impedance grounded generators at one utility in the United States, the element typically detects faults on 90 percent of the stator winding.

The first selectivity method works better for faults closer to the neutral, whereas the second method works better for faults closer to the terminals. Using communications, these two complementary methods can be used to bias the conventional staggered tripping scheme and obtain a selective breaker trip.

VI. APPENDIX

We use the example of a cross-compound unit with a high-impedance grounded HP unit and an ungrounded LP unit sharing a common bus to demonstrate the compensated third-harmonic differential scheme for units with a high degree of VG3 mismatch. The third-harmonic network is shown in Fig. 33. Note that the measurement of the LP unit neutral voltage ($VN3_{LP}$) via a PT is required.

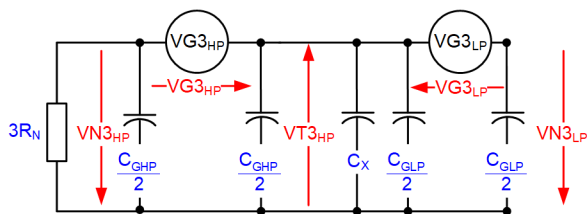


Fig. 33. Equivalent circuit for cross-compound units

Consider the protection for the HP unit. Because it shares a common bus with the LP unit, the approach to maximizing availability is to solve the circuit using a third-harmonic voltage differential principle with the general form of (16) [4]. This method requires knowledge of the ratio of third-harmonic impedances surrounding the protected units, which are typically obtained via measurement of VN3 and VT3. The implementation of the compensated differential scheme is shown in (16) through (22), where 64G2N operates if there is a significant deviation of the terminal and neutral third-harmonic differential values from the expected values.

$$64G2N = RAT_{EQ} \cdot |VT3_{HP}| - |VN3_{HP}| > 64G2NP \quad (16)$$

$$RAT_{EQ} = \left| \frac{VN3_{CALC}}{VT3_{CALC}} \right| \quad (17)$$

$$VN3_{CALC} = VG3_{HP} - VT3_{CALC} \quad (18)$$

$$VT3_{CALC} = VG3_{HP} \cdot \left(\frac{1}{1 + RAT_{HP}} \right) + VG3_{LP} \cdot \left(\frac{1}{1 + RAT_{LP}} \right) \quad (19)$$

$$VG3_{HP} = VT3_{HP} + VN3_{HP} \quad (20)$$

$$RAT_{HP} = \frac{\frac{C_{GHP}}{2} + C_X + C_{GLP}}{\frac{C_{GHP}}{2} + \frac{1}{3j\omega R_N}} \quad (21)$$

$$RAT_{LP} = \frac{\frac{C_{GLP}}{2} + C_X + C_{GHP} + \frac{1}{3j\omega R_N}}{\frac{C_{GHP}}{2} + \frac{1}{3j\omega R_N}} \quad (22)$$

Both RAT_{LP} and RAT_{HP} are relay settings (complex values) associated with the $VN3/VT3$ ratio for the units during healthy operation. $64G2P_{COMP}$ can be set based on similar principles from Scheme B [4], but as the zero-sequence network is stronger with multiple machines sharing a bus, a lower threshold of 1 percent of V_{LN} can be used (instead of 1.75 percent [4]).

This scheme only detects neutral-side faults and is adaptive. Its availability depends on the level of third harmonic produced by the HP unit and the ratio of third harmonic produced by the LP unit with respect to the HP unit.

Using (16) through (22) for an example of $C_{GHP} = 0.3 \mu F$, $C_{GLP} = 0.2 \mu F$, $C_X = 0.1 \mu F$, and $R_N = 2 \text{ k}\Omega$, we obtained Fig. 34. If the protected HP unit in our example produces $VG3_{HP} = 2\% V_{LN}$, then 5 percent coverage to the neutral side is available if $VG3_{LP}$ is less than 6 percent ($2\% V_{LN} \cdot 3.00$).

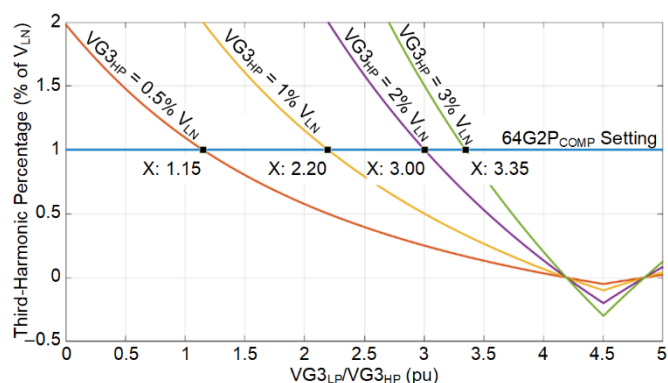


Fig. 34. Availability of the compensated differential scheme as a function of the third-harmonic voltages produced by the HP and LP units

Note that this scheme requires alignment of the VG3 received from the paralleled unit with the VG3 produced by the protected unit. The simplest approach is to communicate the VT3 phasor (which is identical for all units sharing the bus) and then perform the alignment.

The compensated differential scheme can have significantly higher availability than the blocking ratio scheme described in Section II. It requires channel synchronization, and the complexity increases significantly as more units share the bus.

VII. ACKNOWLEDGEMENT

We acknowledge Eric Eastment and Matt Westerdale of the United States Bureau of Reclamation for providing the inspiration and system data for some of this work. We thank Paulo Lima for sharing field data.

VIII. REFERENCES

- [1] N. Klingerman, D. Finney, S. Samineni, N. Fischer, and D. Haas, "Understanding Generator Stator Ground Faults and their Protection Schemes," proceedings of the 69th Annual Conference for Protective Relay Engineers, College Station, TX, April 2016.
- [2] C. V. Maughan, "Incapability of Analog Relay Protection to Detect Generator Stator Winding Ground Failures at Neutral End," proceedings of the 2013 IEEE Electrical Insulation Conference, Ottawa, ON, Canada, June 2013.
- [3] P. Soñez, F. Vicentini, V. Skendzic, M. Donolo, S. Patel, Y. Xia, and R. C. Scharlach, "Injection-Based Generator Stator Ground Protection Advancements," proceedings of the 41st Annual Western Protective Relay Conference, October 2014.
- [4] R. Chowdhury, D. Finney, and N. Fischer, "Comparison of Third-Harmonic Stator Ground Protection Schemes," proceedings of the 14th International Conference on Developments in Power System Protection, Belfast, United Kingdom, March 2018.
- [5] IEEE Power System Relaying Committee, "IEEE Tutorial on the Protection of Synchronous Generators," *IEEE Power & Energy Society*, August 2011. Available: <http://resourcecenter.ieee-pes.org>.
- [6] R. J. Alcantara and F. G. Garcia, "100% Stator Ground Fault Protection – A Comparison of Two Protection Methods," Lund Institute of Technology, 2006. Available: https://www.myprotectionguide.com/uploads/7/3/0/1/73017921/5223_100-statorgroundfaultprotection.pdf.
- [7] T. Bengtsson, A. Gajić, H. Johansson, J. Menezes, S. Roxenborg, and M. Sehlstedt, "Innovative Injection-Based 100% Stator Earth-Fault Protection," proceedings of the 11th IET International Conference on Developments in Power Systems Protection, Birmingham, UK, April 2012.
- [8] N. Klingerman, L. Wright, and B. Cockerham, "Field Experience With Detecting an Arcing Ground Fault on a Generator Neutral Point," proceedings of the 42nd Annual Western Protective Relay Conference, Spokane, WA, October 2015.
- [9] IEEE Standard C37.102, IEEE Guide for AC Generator Protection.
- [10] G. Druml, "Détection de Défauts à la Terre Très Résistants Sur les Réseaux Compensés [Detecting High-Ohmic Earth Faults in Compensated Networks]," *Revue de Electricité et de Electronique*, Vol. 2, Issue 68, January 1996.
- [11] J. Roberts, D. Hou, F. Calero, and H. Altuve, "New Directional Ground-Fault Elements Improve Sensitivity in Ungrounded and Compensated Networks," October 2001. Available: <https://selinc.com>.

IX. BIOGRAPHIES

Ritwik Chowdhury received his Bachelor of Engineering degree from the University of British Columbia and his Master of Engineering degree from the University of Toronto. He joined Schweitzer Engineering Laboratories, Inc. in 2012, where he has served as an application engineer and presently works as a lead power engineer. He has authored several technical papers on power system protection and control. His interests include the analysis and control of generators and their systems, controlled switching, and generator and line protection. He is an active contributor to IEEE PSRC standards development and a registered professional engineer in the province of Ontario.

Dale Finney received his Bachelor of Engineering degree from Lakehead University and his Master of Engineering degree from the University of Toronto. He began his career with Ontario Hydro, where he worked as a protection and control engineer. Currently, Mr. Finney is employed as a principal power engineer with Schweitzer Engineering Laboratories, Inc. Mr. Finney holds more than 10 patents and has authored more than 30 papers in the area of power system protection. He is a member of the main committee and chair of the rotating machinery subcommittee of the IEEE PSRC. He is a senior member of the IEEE and a registered professional engineer in the province of Nova Scotia.

Normann Fischer received a Higher Diploma in Technology, with honors, from Technikon Witwatersrand, Johannesburg, South Africa in 1988; a B.S.E.E., with honors, from the University of Cape Town in 1993; an M.S.E.E. from the University of Idaho in 2005; and a Ph.D. from the University of Idaho in 2014. He joined Eskom as a protection technician in 1984 and was a senior design engineer in the Eskom protection design department for three years. He then joined IST Energy as a senior design engineer in 1996. In 1999, Normann joined Schweitzer Engineering Laboratories, Inc., where he is currently a fellow engineer in the research and development division. He was a registered professional engineer in South Africa and a member of the South African Institute of Electrical Engineers. He is currently a senior member of IEEE and a member of the American Society for Engineering Education.

Jason Young graduated from the University of Waterloo in 2006 with a B.A.Sc. in electrical engineering. He joined Schweitzer Engineering Laboratories, Inc. in 2006, where he currently serves as an application engineer in Smiths Falls, Ontario, Canada. He has authored several technical papers and application guides related to power system protection. His interests include generators, motors, and transformers, and their protection. He is a registered professional engineer in the province of Ontario and an IEEE member.

Veselin Skendzic is a principal research engineer at Schweitzer Engineering Laboratories, Inc. He earned his B.S. in electrical engineering from FESB, University of Split, Croatia; his M.S. from ETF, Zagreb, Croatia; and his Ph.D. from Texas A&M University, College Station, Texas. He has more than 25 years of experience in electronic circuit design and power system protection-related problems. He is an IEEE Fellow, has written multiple technical papers, has over 20 patents, and is actively contributing to IEEE and IEC standards development. Veselin is a member of IEEE PES and IEEE PSRC, and he is a past chair of the PSRC Relay Communications Subcommittee (H).

Subhash Patel received his B.S.E.E. and B.S.M.E. degrees from Maharaja Sayajirao University, Baroda, India, in 1965 and 1966, respectively. He worked for Brown Boveri Company in India before coming to the United States in 1967. He received an M.S. (E.E.) degree from the University of Missouri - Rolla, in 1969 and joined Illinois Power Company in Decatur, Illinois, where he was primarily responsible for power system protection. He was with General Electric from 1979 to 1999, during which time he had various assignments in the field of protection and control as well as gas turbine package power plants. In 1999, Subhash joined Schweitzer Engineering Laboratories, Inc. as a field application engineer and currently is a principal power engineer in Pennsylvania. He is an IEEE Life Member and is involved with IEEE PES, SA, and PSRC SC-J. He is a registered professional engineer in the states of New Hampshire and Illinois and an author of several protective relay conference papers.